



An electrically driven cavity-enhanced source of indistinguishable photons with 61% overall efficiency

A. Schlehahn, A. Thoma, P. Munnely, M. Kamp, S. Höfling, T. Heindel, C. Schneider, and S. Reitzenstein

Citation: [APL Photonics](#) **1**, 011301 (2016); doi: 10.1063/1.4939831

View online: <http://dx.doi.org/10.1063/1.4939831>

View Table of Contents: <http://scitation.aip.org/content/aip/journal/app/1/1?ver=pdfcov>

Published by the [AIP Publishing](#)

Articles you may be interested in

[Mid-infrared silicon-on-sapphire waveguide coupled photonic crystal microcavities](#)

Appl. Phys. Lett. **107**, 081109 (2015); 10.1063/1.4929601

[Ultrafast electrical control of a resonantly driven single photon source](#)

Appl. Phys. Lett. **105**, 051112 (2014); 10.1063/1.4892013

[Electrically driven quantum dot single-photon source at 2GHz excitation repetition rate with ultra-low emission time jitter](#)

Appl. Phys. Lett. **102**, 011126 (2013); 10.1063/1.4774392

[Probing photonic crystals on silicon-on-insulator with Ge/Si self-assembled islands as an internal source](#)

J. Appl. Phys. **99**, 023103 (2006); 10.1063/1.2163007

[APL Photonics](#)

An electrically driven cavity-enhanced source of indistinguishable photons with 61% overall efficiency

A. Schlehahn,¹ A. Thoma,¹ P. Munnely,¹ M. Kamp,² S. Höfling,^{2,3} T. Heindel,^{1,a} C. Schneider,² and S. Reitzenstein¹

¹*Institut für Festkörperphysik, Technische Universität Berlin, 10623 Berlin, Germany*

²*Technische Physik, Physikalisches Institut, Wilhelm Conrad Röntgen Research Center for Complex Material Systems, Universität Würzburg, 97074 Würzburg, Germany*

³*SUPA, School of Physics and Astronomy, University of St. Andrews, St. Andrews KY16 9SS, United Kingdom*

(Received 17 November 2015; accepted 29 December 2015; published online 18 April 2016)

We report on an electrically driven efficient source of indistinguishable photons operated at pulse-repetition rates f up to 1.2 GHz. The quantum light source is based on a p-i-n-doped micropillar cavity with integrated self-organized quantum dots, which exploits cavity quantum electrodynamics effects in the weak coupling regime to enhance the emission of a single quantum emitter coupled to the cavity mode. We achieve an overall single-photon extraction efficiency of $(61 \pm 11) \%$ for a device triggered electrically at $f = 625$ MHz. Analyzing the suppression of multi-photon emission events as a function of excitation repetition rate, we observe single-photon emission associated with $g^{(2)}_{\text{HBT}}(0)$ values between 0.076 and 0.227 for f ranging from 373 MHz to 1.2 GHz. Hong-Ou-Mandel-type two-photon interference experiments under pulsed current injection at 487 MHz reveal a photon-indistinguishability of $(41.1 \pm 9.5) \%$ at a single-photon emission rate of (92 ± 23) MHz. © 2016 Author(s). All article content, except where otherwise noted, is licensed under a Creative Commons Attribution (CC BY) license (<http://creativecommons.org/licenses/by/4.0/>). [<http://dx.doi.org/10.1063/1.4939831>]

Semiconductor quantum dots (QDs) are excellent candidates for the realization of practical quantum light sources¹ for future applications in quantum information technology,² due to the ease of integration into complex micro- and nanophotonic structures and their superior quantum optical properties. In particular, the realization of electrically operated QD-based non-classical light sources is a very active field,³ exhibiting milestones such as the first demonstration of an electrically driven source of single photons⁴ or entangled photon pairs⁵ as well as quantum key distribution experiments.⁶ On the other hand, while high photon-indistinguishabilities have been achieved in numerous Hong-Ou-Mandel (HOM)-type two-photon interference (TPI) experiments under optical pumping using quasi-resonant^{7,8} or strict-resonant^{9,10} excitation schemes, the generation of indistinguishable photons via electrically driven QD devices remains very challenging, due to the intrinsic above-band injection of charge-carriers resulting in an inherent relaxation time jitter as well as dephasing due to electric field noise.¹¹ Bennett *et al.*¹² demonstrated the electrical generation of indistinguishable photons emitted by a QD, by exploiting the quantum-confined Stark-effect to tune the QD emission in and out of the spectral detection window on a time scale short compared to the radiative lifetime of the QD transition. However, this scheme inherently leads to a reduced quantum efficiency of the QD, which limits the single-photon emission rate. In contrast, exploiting the Purcell-effect¹³ in microcavity structures conceptually allows for the generation of photons with short radiative lifetimes at high photon extraction efficiencies under electrical excitation.^{14,15}

^aAuthor to whom correspondence should be addressed. Electronic mail: tobias.heindel@tu-berlin.de



In this work, we realize an efficient, electrically triggered source of indistinguishable single photons. Exploiting the Purcell-effect in electrically contacted QD micropillar cavities operated at excitation repetition rates up to 1.2 GHz, we extract the cavity-enhanced single-photon emission with record-high total efficiencies up to $(61 \pm 11) \%$. Moreover, TPI experiments under pulsed current injection at 487 MHz reveal a photon-indistinguishability of $(41.1 \pm 9.5) \%$ at a single-photon emission rate of (92 ± 23) MHz.

The single-photon source (SPS) used in our experiments is composed of a low-density layer of self-organized InAs QDs embedded in an intrinsic λ -thick GaAs-cavity. An n-type δ -doped layer is introduced close to the QDs to eliminate detrimental dark-state configurations.¹⁶ The cavity is sandwiched between a lower n-doped and an upper p-doped distributed Bragg reflector (DBR) containing 26 and 13 AlAs/GaAs mirror pairs, respectively. The mirror number was optimized for the highest photon extraction efficiencies resulting in moderate Q factors (~ 1300 to 2300) for devices of $2.0 \mu\text{m}$ diameter.¹⁵ Electrically contacted micropillars are processed via electron beam lithography and reactive ion etching¹⁷ to realize the final device illustrated in Fig. 1(a).

The sample is operated in a liquid-helium-flow cryostat at temperatures from 4 K to 30 K. To electrically excite the QD micropillar with high pulse-repetition rates, we use a pulse pattern generator (HP 8133A) with a minimal pulse-width of 50 ps and a maximal repetition rate of 3 GHz. Electrical voltage pulses are applied to the sample via the cryostat's high-frequency capable feedthroughs and a probe needle. A microscope objective (numerical aperture: 0.4), serving as first lens of the detection system, collects and collimates the electroluminescence of the QD-micropillar chip. The collimated emission is spectrally analyzed using a spectrometer enabling a spectral resolution of $25 \mu\text{eV}$. The photon statistics of the sample emission is analyzed by means of photon-autocorrelation measurements in a Hanbury-Brown and Twiss (HBT) setup. To investigate the photon-indistinguishability, HOM-type TPI experiments were performed via an asymmetric Mach-Zehnder interferometer based on polarization-maintaining single-mode fibers. Both the HBT and HOM setup utilize two silicon-based single photon counting modules (SPCMs) and time-correlated single-photon counting (TCSPC) electronics for coincidence measurements (see Ref. 8 for details).

For the experiments, a QD micropillar with a diameter of $2.0 \mu\text{m}$ has been chosen to achieve optimum photon extraction efficiency. Prior to the quantum optical studies, spectral resonance between a single quantum emitter and the cavity mode was induced via temperature tuning. Fig. 1(b) shows micro-electroluminescence (μEL) spectra of a QD micropillar as a function of sample temperature in a contour plot. The device was operated under pulsed electrical current injection at a repetition rate of 373 MHz (pulse-width: 200 ps, DC bias: 1.49 V, pulse-amplitude: 1.38 V). At

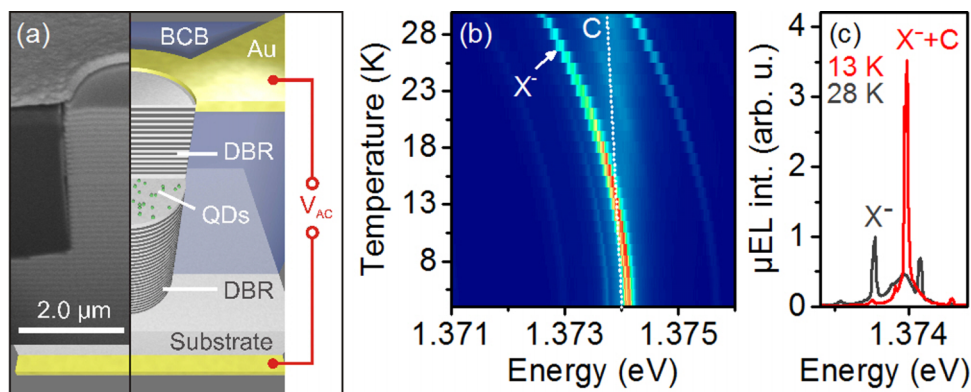


FIG. 1. (a) Illustration of the indistinguishable-photon emitting diode based on a quantum dot (QD) micropillar cavity structure. A cross-sectional scanning electron microscopy image of a fully processed device (left panel) as well as a schematic (right panel) is shown. (b) Contour plot of emission spectra of a QD micropillar vs. sample temperature. The device was operated under pulsed electrical current injection at a repetition rate of 373 MHz. Pronounced Purcell enhancement of the emission is observed by tuning a single QD exciton (X^-) in spectral resonance with the cavity mode (C). (c) μEL spectra of the X^- emission on- (13 K) and off- (28 K) resonance with the cavity mode C.

a temperature of 28 K, the emission of a singly negatively charged exciton state X^- is observed at the low energy side of the cavity mode C ($Q = 2100 \pm 100$). Decreasing the temperature results in a spectral shift of the X^- emission towards the cavity mode at higher energies, accompanied by a pronounced increase of the emission intensity due to the Purcell-effect. The maximum Purcell-induced emission enhancement is reached at spectral resonance with the cavity mode at a temperature of 13 K. We have deliberately chosen a QD resonance at rather low temperatures, as phonon-induced pure dephasing is known to severely affect the photon-indistinguishability.^{18,19} To determine the Purcell-factor F_P from the μ EL spectra, we extracted the integrated emission intensity of the X^- state as a function of the spectral detuning to the cavity mode and applied formula (10) from Ref. 20, yielding $F_P = 3.2 \pm 0.4$.

To gain insight into the photon statistics of the QD emission, we performed measurements of the second-order photon-autocorrelation $g^{(2)}(\tau)$. For this purpose, the spectrally filtered emission of the resonantly coupled X^- state (cf. Fig. 1(c)) was coupled to the HBT setup. The resulting coincidence histogram of $g^{(2)}_{\text{HBT}}(\tau)$ is presented in the upper panel of Fig. 2(a). Electrically triggered single-photon emission of the coupled QD-cavity system is reflected in the strongly reduced number of coincidences at zero time delay ($\tau = 0$). At finite τ , coincidence maxima occur at a periodicity, corresponding to the pulse-repetition rate of 373 MHz. For a quantitative evaluation of the suppression of two-photon emission events, we fitted the experimental data with a sequence of equidistant photon pulses, each represented by the convolution of a two-sided exponential (decay-time-constant τ_D) with a Gaussian of 350 ps width (full-width at half-maximum), accounting for the HBT's timing resolution. Assuming a constant area A of the pulses at finite time delay, $g^{(2)}_{\text{HBT}}(0)$ is expressed by the ratio A_0/A , where A_0 corresponds to the area of the zero-delay peak. The fitted model function (red line in Fig. 2(a)) reveals an antibunching of $g^{(2)}_{\text{HBT}}(0) = 0.076 \pm 0.014$, demonstrating triggered single-photon emission with excellent suppression of multi-photon emission events. The combined detection rate of the SPCMs amounts to 240 kHz. Taking the detection efficiency of the HBT setup $\eta_{\text{HBT}} = (2.45 \pm 0.29) \times 10^{-3}$ (measured according to Ref. 21), we are able to deduce

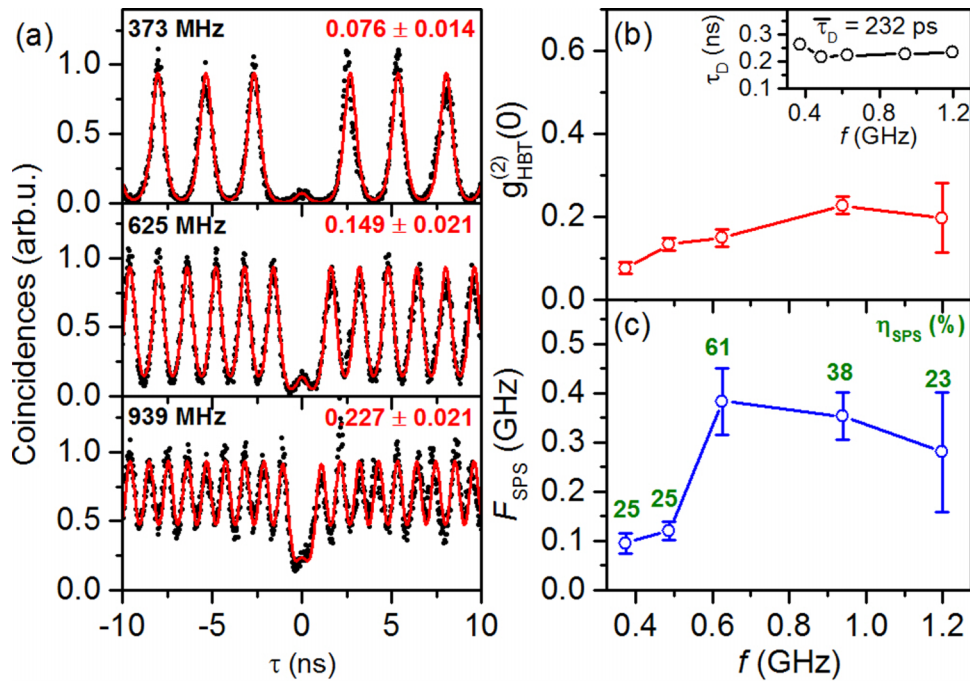


FIG. 2. Photon-autocorrelation analysis (HBT configuration) of an electrically triggered coupled QD-cavity device. (a) Exemplary coincidence histograms for increasing excitation repetition rate f . Red lines represent a fit to the data assuming a mono-exponential radiative decay and considering the timing resolution of the detection system. Extracted $g^{(2)}_{\text{HBT}}(0)$ values (highlighted in red) are depicted in (b) as a function of f . Inset: extracted decay time τ_D of the QD transition. (c) Single photon emission rate F_{SPS} and the corresponding overall efficiency η_{SPS} vs. f .

the photon flux F emitted into the first lens of the setup to $F = 240 \text{ kHz}/\eta_{\text{HBT}} = (99 \pm 11) \text{ MHz}$. Correcting for two-photon emission events according to Ref. 22, we obtain the single-photon emission rate $F_{\text{SPS}} = F \times (1 - g_{\text{HBT}}^{(2)}(0))^{1/2} = (95 \pm 20) \text{ MHz}$, which corresponds to an overall efficiency of the SPS of $\eta_{\text{SPS}} = F_{\text{SPS}}/f = (25.4 \pm 5.5) \%$. To evaluate the performance of our device at the highest modulation frequencies, we gradually increased the excitation repetition rate. Here, DC bias and pulse-amplitude have been adjusted slightly for each excitation repetition rate ($\leq 10\%$ change of the above mentioned parameters), in order to optimize the signal-to-background ratio. The middle and lower panels of Fig. 2(a) exemplarily depict HBT measurements at modulation speeds of 625 MHz and 939 MHz together with a fit to the experimental data. Both histograms reveal strong antibunching and clearly attest single-photon emission of the QD-cavity system at ultra-high repetition rates. As seen from Fig. 2(b), where the extracted $g_{\text{HBT}}^{(2)}(0)$ values are presented as a function of modulation speed, the suppression of two-photon emission events remains well below 0.25 in the entire frequency range. Only a slight increase in $g_{\text{HBT}}^{(2)}(0)$ is observed, which most probably results from increased contributions of uncorrelated background emitters non-resonantly feeding the cavity mode^{23–25} due to an f -dependent current density distribution within the QD-layer (cf. discussion of Fig. 2(c)). While at 625 MHz the coincidence maxima still remain well separated in time, they show a significant overlap at 939 MHz, as the modulation speed gets comparable to the inverse decay time of the QD state ($1/\tau_{\text{D}} = 4.3 \text{ GHz}$). Here, the QD decay time τ_{D} of $(232 \pm 18) \text{ ps}$ has been extracted from the fit to the HBT measurements and is found to be almost constant over the investigated frequency range, as expected. Fig. 2(c) displays the deduced single-photon emission rate F_{SPS} into the first lens as a function of modulation speed f . The maximal rate of $F_{\text{SPS}} = (383 \pm 68) \text{ MHz}$ is achieved at a modulation speed of 625 MHz, associated with a combined detected rate at the SPCMs of 1 MHz. The associated overall efficiency of $\eta_{\text{SPS}} = F_{\text{SPS}}/f = (61 \pm 11) \%$ is the highest efficiency reported for electrically triggered SPSs so far and represents a significant improvement compared to our previous work of Ref. 15. Further increasing the modulation speed f to 939 MHz, F_{SPS} and η_{SPS} first stagnate and finally at 1.2 GHz slightly decrease. Interestingly, the highest measured overall efficiency of $(61 \pm 11) \%$ compares well with the estimated photon extraction efficiency²⁶ of $\eta_{\text{ext}} = Q/Q_{2\text{D}} \times F_{\text{P}}/(F_{\text{P}} + 1) = 53\%$ of the present device, with experimentally determined values for Q and F_{P} from above and $Q_{2\text{D}} = 3000$,¹⁵ indicating that the electrical injection efficiency into the QD is very high. The observation of a frequency-dependent overall efficiency η_{SPS} further suggests an f -dependent current injection efficiency into the QD. A possible explanation for this effect, which is typically observed for this type of structure,²⁷ is a frequency-dependent spatial current density distribution within the QD layer. The same effect possibly also causes the f -dependence of $g_{\text{HBT}}^{(2)}(0)$ (cf. Fig. 2(b)), which reduces the efficiency at high repetition rates due to the correction for two-photon emission events.

Next, the photon-indistinguishability is addressed by TPI experiments. For this purpose, the cavity-enhanced X^- emission electrically triggered at 487 MHz is coupled to the HOM setup, where the repetition rate has been chosen to coarsely match the delay in the interferometer while a fine adjustment was performed via a variable fiber-delay. Fig. 3(a) displays the obtained coincidence histogram of the two-photon detection events at the two outputs of the HOM interferometer for

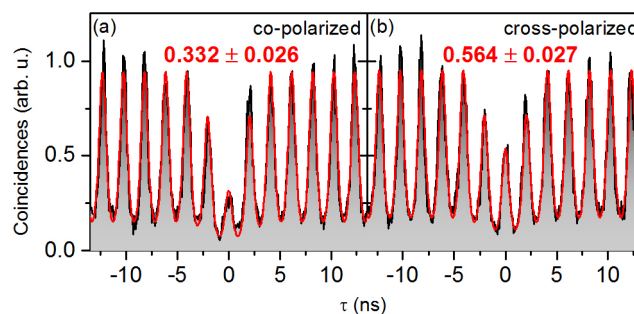


FIG. 3. Hong-Ou-Mandel-type two-photon interference (TPI) experiment on the single-photon stream emitted by our device at a repetition rate of 487 MHz. Experimental data for co-polarized (a) and cross-polarized (b) measurement configuration are presented as well as the corresponding fits (red lines), revealing a TPI visibility of 41%.

co-polarized measurement configuration. Quantum-mechanical TPI manifests in a strongly reduced number of coincidences at $\tau = 0$, if compared to the measurement in cross-polarized configuration (cf. Fig. 3(b)). To quantitatively extract the visibility of TPI, i.e., the mean photon wave-packet overlap, we fitted the experimental data according to the model applied in Fig. 2(a). Additionally, the peak areas at $\tau = \pm 2.062$ ns have been fixed to the theoretically expected value of 0.75A, where A corresponds to the area of the peaks at $|\tau| > 2.062$ ns in this case.¹² The peak area ratio of $3/4$ can thereby be deduced by combinatorics, assuming an asymmetric Mach-Zehnder interferometer with 50:50 beam-splitters and calculating the possible pulse-configurations leading to coincidences at finite τ . From the extracted relative peak areas A_0/A , we gain values of $g_{\parallel}^{(2)}(0) = 0.332 \pm 0.026$ and $g_{\perp}^{(2)}(0) = 0.564 \pm 0.027$ for the antibunching in co- and cross-polarized measurement configurations, respectively. The corresponding visibility of two-photon interference yields $V = (g_{\perp}^{(2)}(0) - g_{\parallel}^{(2)}(0))/g_{\perp}^{(2)}(0) = (41.1 \pm 9.5) \%$. The X^- state showed a combined detection rate at the SPCMs of the HOM setup of $R_{\text{det}} = (25.5 \pm 1.5)$ kHz, which corresponds to a flux $F_{\text{ISPS}} = R_{\text{det}} \times (1 - g_{\text{HBT}}^{(2)}(0))^{1/2} / \eta_{\text{HOM}} = (92 \pm 23)$ MHz of single photons with 41% TPI visibility. Here, we corrected F_{ISPS} for multi-photon emission events present in the actual HOM experiment by independently measuring $g_{\text{HBT}}^{(2)}(0) = 0.139 \pm 0.030$ and took into account the detection efficiency of the HOM setup ($\eta_{\text{HOM}} = (0.258 \pm 0.030) \times 10^{-3}$). The corresponding overall efficiency is $(18.8 \pm 4.6) \%$ and equals the product of the charge-carrier injection efficiency and the estimated photon extraction efficiency ($\eta_{\text{ext}} \sim 53\%$, see above), where η_{ext} depends only on the cavity parameters and the Purcell factor. Thus, we estimate a charge-carrier injection efficiency of $\sim 35\%$ ($=\eta/\eta_{\text{ext}}$) which limits the efficiency at this specific working point. Although the TPI visibility of $(41.1 \pm 9.5) \%$ observed in our experiment is quite remarkable for non-resonant excitation schemes,²⁸ it is still significantly lower compared to experiments using quasi- or strict-resonant optical excitation, where visibilities close to unity have been reported.^{7,10,29,19} A possible reason is the finite time jitter resulting from the phonon-mediated relaxation of charge carriers from the bulk material into the QDs, leading to a jitter in the arrival time at the HOM beam splitter thus reducing the photon wave-packet overlap. This time jitter can be reduced, by exploiting advanced above band electrical excitation schemes^{12,30} at the cost of lower device efficiencies. Additionally, dephasing due to electric field noise generated by fluctuating charge traps reduces the degree of TPI.¹¹ Thus, we conclude that resonant electrical injection schemes^{31–33} or on-chip optical excitation schemes³⁴ might be useful to simultaneously achieve high photon-indistinguishabilities and high efficiencies in an integrated device approach.

In summary, we realized an ultra-bright electrically triggered source of indistinguishable photons based on a QD micropillar cavity operated at a modulation speed of up to 1.2 GHz. Due to the pronounced Purcell-effect, we achieve an overall efficiency of $(61 \pm 11) \%$ at 625 MHz. Additionally, HOM-type TPI experiments under pulsed current injection at 487 MHz reveal a photon-indistinguishability of $(41.1 \pm 9.5) \%$ at a single-photon emission rate of (92 ± 23) MHz. The presented results are promising with respect to the realization of practical and highly integrated quantum light sources for applications in quantum information technology.

The authors gratefully acknowledge expert sample growth by M. Lerner as well as sample processing by M. Emmerling and A. Wolf. This work was financially supported by the German Research Foundation (DFG) under Grant Nos. RE2974/9-1 and SCHN1376/1-1 as well as the German Federal Ministry of Education and Research (BMBF) through the VIP-project ‘‘QSOURCE.’’

¹ G.-C. Shan, Z.-Q. Yin, C. Shek, and W. Huang, *Front. Phys.* **109**, 170 (2014).

² J.-W. Pan, Z.-B. Chen, C.-Y. Lu, H. Weinfurter, A. Zeilinger, and M. Zukowski, *Rev. Mod. Phys.* **84**, 777 (2012).

³ A. Boretti, L. Rosa, A. Mackie, and S. Castelletto, *Adv. Opt. Mater.* **3**, 1012 (2015).

⁴ Z. Yuan, B. E. Kardynal, R. M. Stevenson, A. J. Shields, C. J. Lobo, K. Cooper, N. S. Beattie, D. A. Ritchie, and M. Pepper, *Science* **295**, 102–105 (2002).

⁵ C. L. Salter, R. M. Stevenson, I. Farrer, C. A. Nicoll, D. A. Ritchie, and A. J. Shields, *Nature* **465**, 594 (2010).

⁶ T. Heindel, C. A. Kessler, M. Rau, C. Schneider, M. Fürst, F. Hargart, W. M. Schulz, M. Eichfelder, R. Rossbach, S. Nauerth, M. Lerner, H. Weier, M. Jetter, M. Kamp, S. Reitzenstein, S. Höfling, P. Michler, H. Weinfurter, and A. Forchel, *New J. Phys.* **14**, 083001 (2012).

⁷ C. Santori, D. Fattal, J. Vučković, G. S. Solomon, and Y. Yamamoto, *Nature* **419**, 594 (2002).

⁸ M. Gschrey, A. Thoma, P. Schnauber, M. Seifried, R. Schmidt, B. Wohlfeil, L. Krüger, J. H. Schulze, T. Heindel, S. Burger, F. Schmidt, A. Strittmatter, S. Rodt, and S. Reitzenstein, *Nat. Commun.* **6**, 7662 (2015).

- ⁹ S. Ates, S. M. Ulrich, S. Reitzenstein, A. Löffler, A. Forchel, and P. Michler, *Phys. Rev. Lett.* **103**, 167402 (2009).
- ¹⁰ Y.-M. He, Y.-J. Wei, D. Wu, M. Atatüre, C. Schneider, S. Höfling, M. Kamp, C.-Y. Lu, and J.-W. Pan, *Nat. Nanotechnol.* **8**, 213 (2013).
- ¹¹ C. Santori, D. Fattal, J. Vuckovic, G. S. Solomon, and Y. Yamamoto, *New J. Phys.* **6**, 89 (2004).
- ¹² A. J. Bennett, R. B. Patel, A. J. Shields, K. Cooper, P. Atkinson, C. A. Nicoll, and D. A. Ritchie, *Appl. Phys. Lett.* **92**, 193503 (2008).
- ¹³ E. M. Purcell, *Phys. Rev.* **69**, 681 (1946).
- ¹⁴ D. J. P. Ellis, A. J. Bennett, S. J. Dewhurst, C. A. Nicoll, D. A. Ritchie, and A. J. Shields, *New J. Phys.* **10**, 043035 (2008).
- ¹⁵ T. Heindel, C. Schneider, M. Lermer, S. H. Kwon, T. Braun, S. Reitzenstein, S. Höfling, M. Kamp, and A. Forchel, *Appl. Phys. Lett.* **96**, 011107 (2010).
- ¹⁶ S. Strauf, N. G. Stoltz, M. T. Rakher, L. A. Coldren, P. M. Petroff, and D. Bouwmeeste, *Nat. Photonics* **1**, 704–708 (2007).
- ¹⁷ C. Böckler, S. Reitzenstein, C. Kistner, R. Debusmann, A. Löffler, T. Kida, S. Höfling, A. Forchel, L. Grenouillet, J. Claudon, and J. M. Gérard, *Appl. Phys. Lett.* **92**, 091107 (2008).
- ¹⁸ S. Varoutsis, S. Laurent, P. Krämper, A. Lemaître, I. Sagnes, I. Robert-Philip, and I. Abram, *Phys. Rev. B* **72**, 041303(R) (2005).
- ¹⁹ A. Thoma, P. Schnauber, M. Gschrey, M. Seifried, J. Wolters, J.-H. Schulze, A. Strittmatter, S. Rodt, A. Carnele, A. Knorr, T. Heindel, and S. Reitzenstein, *Phys. Rev. Lett.* **116**, 033601 (2016).
- ²⁰ M. Munsch, A. Mosset, A. Auffèves, S. Seidelin, J. P. Poizat, J.-M. Gérard, A. Lemaître, I. Sagnes, and P. Senellart, *Phys. Rev. B* **80**, 115312 (2009).
- ²¹ A. Schlehahn, M. Gaafar, M. Vaupel, M. Gschrey, P. Schnauber, J.-H. Schulze, S. Rodt, A. Strittmatter, W. Stolz, A. Rahimi-Iman, T. Heindel, M. Koch, and S. Reitzenstein, *Appl. Phys. Lett.* **107**, 041105 (2015).
- ²² M. Pelton, C. Santori, J. Vučković, B. Zhang, G. S. Solomon, J. Plant, and Y. Yamamoto, *Phys. Rev. Lett.* **89**, 233602 (2002).
- ²³ D. Press, S. Götzinger, S. Reitzenstein, C. Hofmann, A. Löffler, M. Kamp, A. Forchel, and Y. Yamamoto, *Phys. Rev. Lett.* **98**, 117402 (2007).
- ²⁴ K. Hennessy, A. Badolato, M. Winger, D. Gerace, M. Atatüre, S. Gulde, S. Fält, E. L. Hu, and A. Imamoglu, *Nature* **445**, 896 (2007).
- ²⁵ S. Ates, S. M. Ulrich, A. Ulhaq, S. Reitzenstein, A. Löffler, S. Höfling, A. Forchel, and P. Michler, *Nat. Photonics* **3**, 724 (2009).
- ²⁶ W. Barnes, G. Björk, J. Gérard, P. Jonsson, J. Wasey, P. Worthing, and V. Zwiller, *Eur. Phys. J. D* **18**, 197–210 (2002).
- ²⁷ T. Heindel, C. Schneider, M. Lermer, S. Höfling, S. Reitzenstein, L. Worschech, and A. Forchel, *J. Phys.: Conf. Ser.* **245**, 012005 (2010).
- ²⁸ E. B. Flagg, A. Muller, S. V. Polyakov, A. Ling, A. Migdall, and G. S. Solomon, *Phys. Rev. Lett.* **104**, 137401 (2010).
- ²⁹ S. Unsleber, D. P. S. McCutcheon, M. Dambach, M. Lermer, N. Gregersen, S. Höfling, J. Mörk, C. Schneider, and M. Kamp, *Phys. Rev. B* **91**, 075413 (2015).
- ³⁰ F. Hargart, C. A. Kessler, T. Schwarzbäck, E. Koroknay, S. Weidenfeld, M. Jetter, and M. Michler, *Appl. Phys. Lett.* **102**, 011126 (2013).
- ³¹ L. Turyanska, A. Baumgartner, A. Chaggar, A. Patanè, L. Eaves, and M. Henini, *Appl. Phys. Lett.* **89**, 092106 (2006).
- ³² A. Baumgartner, E. Stock, A. Patanè, L. Eaves, M. Henini, and D. Bimberg, *Phys. Rev. Lett.* **105**, 257401 (2010).
- ³³ M. J. Conterio, N. Sköld, D. J. P. Ellis, I. Farrer, D. A. Ritchie, and A. J. Shields, *Appl. Phys. Lett.* **103**, 162108 (2013).
- ³⁴ P. Munnely, T. Heindel, M. M. Karow, S. Höfling, M. Kamp, C. Schneider, and S. Reitzenstein, *IEEE J. Sel. Top. Quantum Electron.* **21**, 1–9 (2015).